Atlas Journal of Materials Science 2 (1): 54–59, 2015
doi: 10.5147/ajms.2015.0165

Preparation and Characterization of Molybdenum Thin Films by Direct-Current Magnetron Sputtering

Shih-Fan Chen[1], Shea-Jue Wang[1*], Win-Der Lee[2], Ming-Hong Chen[1], Chao-Nan Wei[3], and Huy-Yun Y. Bor[3]

[1] Department of Materials and Minerals Resources Engineering, National Taipei University of Technology, Taipei 106, Taiwan; [2] Department of Electrical Engineering, Lee-Ming Institute of Technology, New Taipei City 24305, Taiwan; [3] Materials & Electro-Optics Research Division, Chung-Shan Institute of Science & Technology, Taoyuan 325, Taiwan.

Received: December 7, 2014 / Accepted: March 15, 2015

Abstract

The back contact electrode with molybdenum (Mo) thin film is crucial to the performance of Cu(In, Ga)Se_2 solar cells. In this research, Mo thin films were fabricated by direct current sputtering to attain low-resistivity molybdenum films on soda-lime glass substrates with good adhesion. The films were sputtered onto substrates in 500 nm thickness and nominally held at room temperature with deposition conditions of power and working pressure. Low resistivity (17-25 μΩ·cm) of bi-layer molybdenum thin films were achieved with combination of top layer films deposited at 300 W with different working pressure, and bottom fixing layer film deposited at 300 W with 2.5 mTorr which adhered well on glass. Films were characterized the electrical properties, structure, residual stress, morphology by using the Hall-effect Measurement, X-ray Diffraction, and Field-Emission Scanning Electron Microscopy, respectively, to optimize the deposition conditions.

Keywords: Back contact electrode; Bi-layer; Molybdenum; Thin film; Solar cell.

Introduction

Solar cells are one of the important alternative energy technologies to alleviate the demands on the fossil and nuclear energy (Dresselhaus et al. 2001). The solar cells fabricated with various thin film materials on the substrate, such as the glass, metal foil or plastic with cheap production offer potential applications in our daily life technologies. The thin film solar cells may be classified as cadmium telluride, copper indium gallium diselenide, amorphous and polycrystalline silicon, organics, polymer and dye sensitive materials (Green et al. 2011).

From all current solar cell technologies, the one with more industrial interest and the capability of producing gigawatt per year is Cu(In,Ga)Se2 (CIGS) based solar cells (Dhere 2007) . Remarkable progress has been made in the development of conversion efficiency of CIGS cells on glass substrates that is beyond 20% (Jackson et al. 2011). However, transferring CIGS PV modules from lab to manufacturing scale has been much more challenging for the requirements of higher module efficiency, columnar CIGS structures deposited by robust process for high efficiency cells and modules, thinner absorber layer (≤ 1 μm), and CIGS absorber film stoichiometry and uniformity over large areas, refer to the paper by Singh et al. (2010).

The device structure of CIGS cell comprises of a substrate, metal back contact layer, CIGS (absorber layer), CdS (buffer layer), ZnO, and Al2O3-doped ZnO (window layer), in which each layer has significant effects on the cell performance (Wu et al. 2012). The resistivity of back contact can affect the series resistance of the cell circuit to deteriorate the fill factor of solar cell. The other beneficial factors for back contact layer in CIGS

* Corresponding author: sjwang@ntut.edu.tw

cell require good adhesion, smooth roughness, chemically inert with the materials deposited on top and high reflectivity of film on substrate (Jubault et al., 2011). Moreover, the back contact layer serves as a diffusion barrier hindering the diffusion of impurities from the substrate into the absorber (Yoon et al., 2011). Molybdenum (Mo) is a metal widely used as a back contact for CIGS solar cells, which can be deposited as thin films with a good resistivity, a good adhesion and fair smoothness. It does not react with Cu, Ga or In. A MoSe2 layer was formed during the CIGS process to minimize the negative effect of Schottky barrier at the CIGS/Mo interface and enhance the ohmic contact behavior on solar-cell performances (Hsiao et al. 2013). With 0.1 at.% Na incorporated into the CIGS absorber layer, the performance of CIGS solar cells using soda-lime glass (SLG) substrates can be improved. The Mo films allow the diffusion of Na from the SLG during CIGS growth process.

Mo films on CIGS have been synthesized using sputter deposition (Huang et al. 2013; Wang et al. 2014), e-gun evaporation (Hoffman et al. 1991). However, most of research works take the sputtering method as the major deposition way for the target of refractory metal with high melting temperatures and large area process. In addition, controlling gas atmosphere and substrate temperature for the quality of films is more feasible than for other deposition techniques. In this work, we systematically investigated the influence of deposition parameters such as the direct current (DC) power and working gas pressure on structural, morphological, and electrical properties of molybdenum films. With through understanding the single layer of Mo films on SLG, bilayer Mo film on SLG were studied to explore the feasible conditions of stacked films for CIGS solar cell.

Experimental Procedure

The Mo films were deposited onto SLG substrates (EAGLE 2000, Corning Incorporated) by the DC magnetron sputtering of a high-purity molybdenum target (3 inch in diameter, 99.99%; KaoDuen Technology Corp., Taiwan) in a vacuum chamber with a base pressure $< 7\times10^{-6}$ Torr. Pure argon (99.99 %) was used as sputtering gas to deposit the Mo films. The working distance between target and substrate is 9 cm. Before the deposition, the glass substrate with a dimension of 2.54 mm × 2.54 mm × 0.7 mm was cleaned for 15 minutes in an ultrasonic cleaner with a solution comprising of acetone, methyl-alcohol, and DI water, and dried with a nitrogen blower. The films were sputtered onto the glass substrates at room temperature. Before deposition, the target was cleaned by sputtering for about 10 minutes to minimize the contamination of the target during the opening of the chamber. The deposition parameters of fabricating single layer of Mo films are listed in Table 1. The thickness of films is kept at about 500 nm to avoid blurring the measurement of electrical characteristics. After the results of studying single layer film, the deposition conditions of the second films for a bilayer stack will be on one of the better condition of single layer film data.

Crystal structure of the films was examined and crystallized phases in films were identified by a thin film XRD (Rigaku D/max-B) with monochromatic Cu Kα radiation, and microstructural analyses of the top and cross-section of the films were conducted by a FESEM (field-emission scanning electron microscope, HITACHI S-4700). The deposition rates of the films were calculated by thickness data measured from SEM results, and electrical resistivity of Mo films was measured using a 4-point probe method with KEITHLEY 2400. Adhesion to the substrate after deposition was tested by Scotch tape test method. Carrier mobility of the Mo films was investigated by a Hall-effect measurement system (ECOPIA HMS-3000 ver. 3.5). In addition, samples were scratched to a rectangle shape and adhesive tape stripes of the same length were glued on the scratched films and stripped with approximately equal amounts of force.

Table 1. Sputtering parameters for depositing single layer of Mo thin films.

Power (W)	200	250	300	350	400	450	500
Pressure (mTorr)	2.5	5	10	15	20		
Ar flow (Sccm)	30						
Thickness (nm)	500						
Deposition time(min)	14	10.9	8.1	7	6.1	5.3	5

Results and Discussion

Figure 1 shows XRD patterns of the Mo films prepared at 10 mTorr and DC sputtering power, all films showed a typical body-centered cubic (BCC) Mo structure (space group $Im\bar{3}m$), with a major peak (40.5°) corresponding to an orientation along (110) direction. The intensities of the XRD peak indicated that the films grew with a preferred orientation along the (110) plane as increasing sputtering power, a typical feature of the Mo films deposited by sputtering processes at room temperature (Assmann et al. 2005). Stress of the deposited Mo films on glass is crucial for the application on CIGS cell. The residual stresses in the Mo sample determined by the Voigt fit for the XRD measurement are shown in Figure 2, which exhibits the effect of sputtering power condition on the Mo films stress. The compressive stress increases as the power increases from 300 W to 500 W. The residual stress in films changes from tensile to compressive, which was dependent of voids in crystalline lattices and grain boundaries bombarded by the energetic ions (Thornton et al 1989).

Figure 3 shows top view SEM images of the Mo films prepared at a 10 mTorr and the different working powers from 200 W to 500 W. Grains with small pyramidal shape were observed in the sample with lower sputtering powers. With increasing the sputtering power, the grains turn to mackerel shape with larger size. The films deposited at higher powers display a larger packed grain microstructure with closed boundaries and less voids, because the Mo particles have a longer free path way and a higher kinetic energy during the deposition (Gordillo 1998). Table 2 presents the electrical resistivity and sheet resistance of the Mo films prepared at 10 mTorr with different DC sputtering power. The electrical resistivity and sheet resistance of the Mo film show same decreasing behavior with increasing sputtering power. Both of them are decreased as increasing the sputtering power, similar to the work by Li et al. (2011). Table 3 presents the resistivities and sheet resistance of Mo films prepared at 300 W and different working pressure. High working pressure in sputtering does not favor the electrical properties

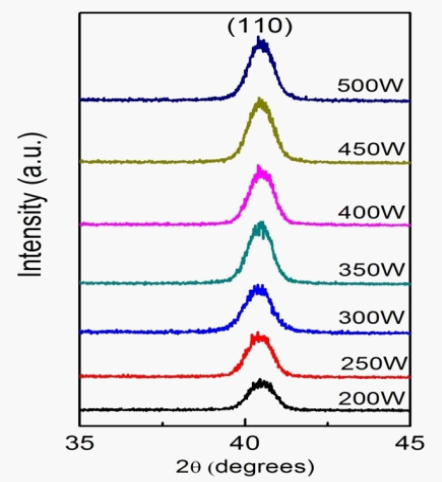

Figure 1. XRD patterns of characteristic (110) peaks of Mo films prepared at 10 mTorr and different DC sputtering powers.

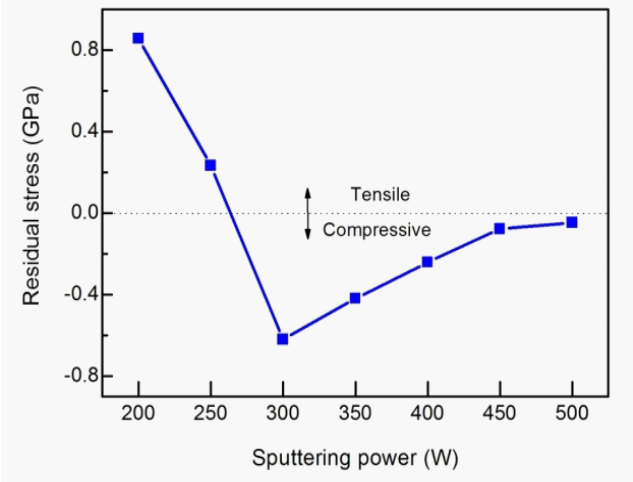

Figure 2. Residual stress vs. sputtering power of Mo thin films at 10 mTorr were determined by XRD.

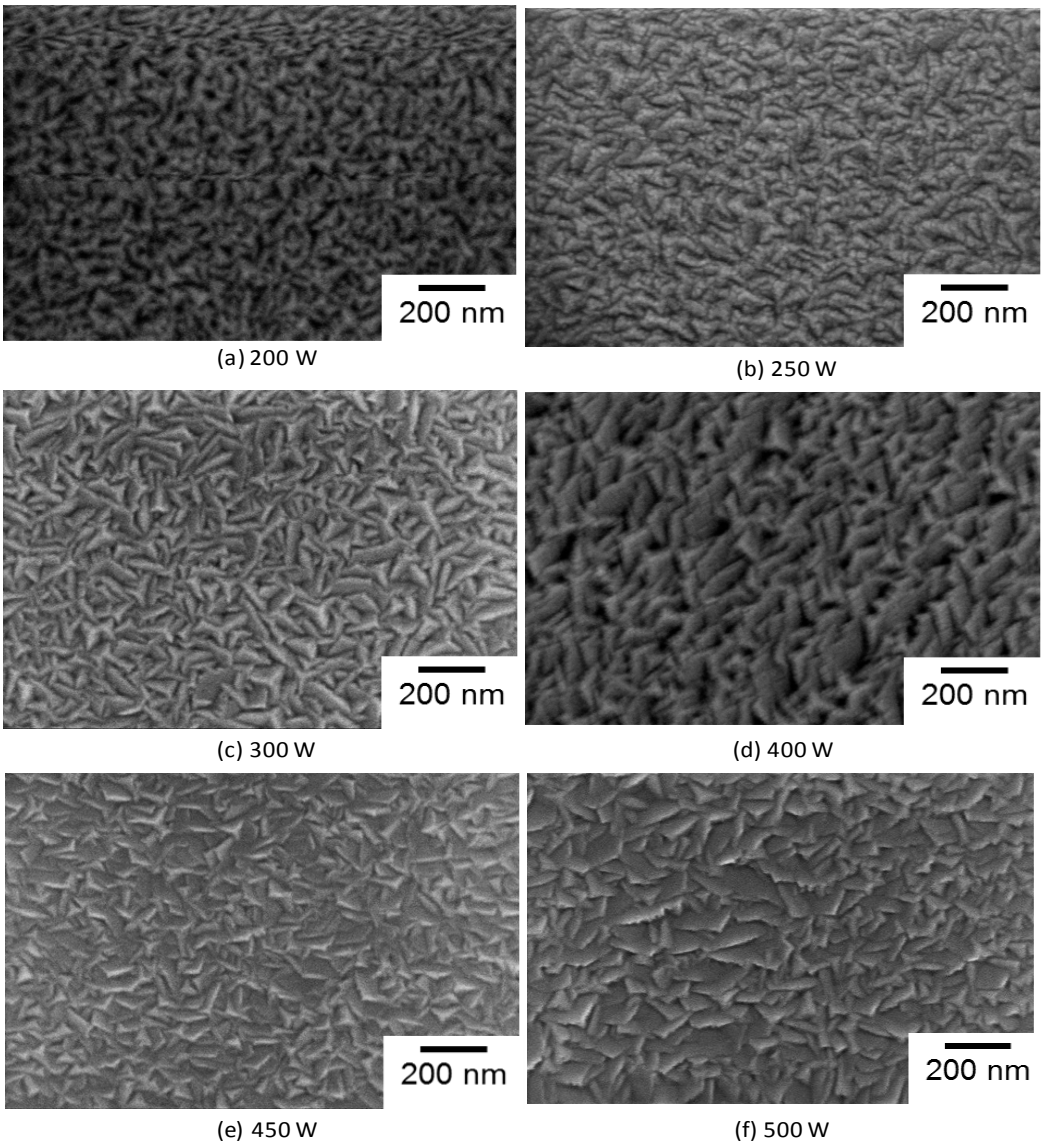

Figure 3. Top surface SEM images of Mo films prepared at 10 mTorr and different sputtering power.

Table 2. Resistivities and sheet resistance of Mo films prepared at 10 mTorr and different sputtering power.

Power (W)	Resistivity (μΩ·cm)	Sheet resistance (Ω/□)
200	78.09	1.698
250	60.23	0.844
300	49.77	0.775
350	49.51	0.741
400	38.95	0.415
450	35.48	0.364
500	31.35	0.296

Table 3. Resistivities and sheet resistance of Mo films prepared at 300 W and different working pressure.

Pressure (mTorr)	Resistivity (μΩ·cm)	Sheet Resistance (Ω/□)
2.5	16.93	0.32
5	25.89	0.51
10	31.03	0.62
15	41.95	0.81
20	92.28	1.85

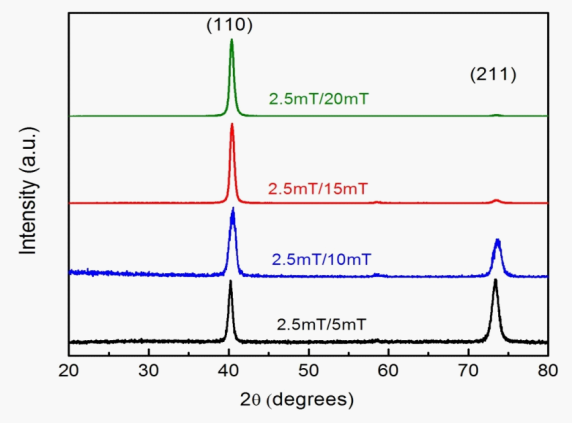

Figure 4. XRD patterns of of Mo films prepared at 300 W and different DC working pressure.

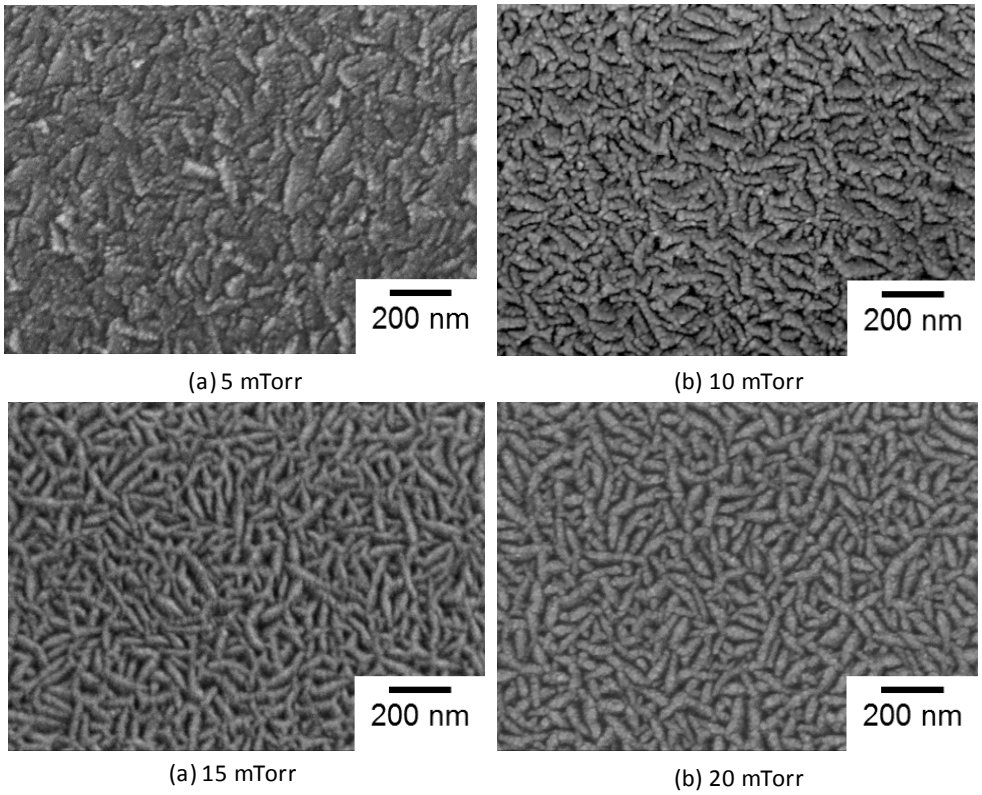

Figure 5. Top surface SEM images of bilayer Mo films while top layer films prepared at 300 W and different working pressure.

Table 4. Resistivities and sheet resistance of bilayer Mo films with the top layer films prepared at 300 W and different working pressure.

(bottom/top) (mTorr)	Resistivity (μΩ·cm)	Sheet resistance (Ω/□)
2.5/5	17.14	0.17
2.5/10	20.84	0.19
2.5/15	23.73	0.22
2.5/20	24.65	0.23

of the Mo films. As compared with Tables 2 and 3, the minimum resistivity of single layer Mo films deposited with 300 W and 2.5 mTorr is about 17 μΩ·cm.

When the sputtering power rises, the atomic energy of ion bombardment of molybdenum deposited on the substrate increases. Mo film surface morphology, such as small pyramids with pore membrane structure, transform to larger dense triangular cone structure.

Owing to the poor adhesion of the low resistive Mo films on the SLG, the bilayer stack structure of Mo films is employed in the application of CIGS cell. The top layer of a bilayer Mo films (500 nm) is fixed at deposition conditions of 300 W and 2.5 mTorr for the lowest resistivity for minimizing ohmic contact issue of CIGS absorber films. The bottom layer of Mo thin films is fixed to 500 nm and deposited at 300 W and different working pressures. Figure 4 shows the XRD patterns of of Mo films prepared at 300 W and different DC working pressure. The intensity of (211) peaks are decreased with increasing the working pressure. Figure 5 shows the top surface SEM images of bilayer Mo films while top layer films prepared at 300 W and different working pressure. The shape of the grains seem to be different from the morpholorgy of single-layer Mo films. Long sharp columnar grains appear at higher working pressure. A higher working gas pressure in sputtering will change the quality of the top layer film (Moons e al. 1993). Table 4 shows the resistivities and sheet resistance of bilayer Mo films while top layer films prepared at 300 W and different working pressures. As compared with the Figure 5, less packing density of columnar grains will induce more scattering events for carrier motion.

Increasing the sputtering power of molybdenum thin films from 200 W to 500 W at 10 mTorr yields a decrease in resistivity from 78.09 μΩ·cm to 31.35 μΩ·cm, possibly because the residual stress changes from tensile to compressive stress. Likewise, films with the working pressure increased from 2.5 mTorr to 20 mTorr at 300 W shows increased resistivity from 16.93 μΩ·cm to 92.28 μΩ·cm while the residual stress of Mo films is compressive stress, except for tensile stress observed at 2.5 mTorr.

Conclusions

The single layer and bilayer Mo films were successfully prepared using DC sputtering. The residual stress of the single layer films changed from tensile to compressive when the sputtering power is reduced. The lowest resistivity of single layer Mo film was about 17 μΩ·cm, which acted as a top contact layer of bilayer electrode. The resistivity of bilayer Mo films with bottom layer deposited at a sputtering power of 300 W and various working pressures showed the resistivity around 17-25 μΩ·cm that was lower than results by Wang et al. (2014). These results indicated that the bilayer Mo films prepared by the study could be used as back metal contacts in CIGS solar cells.

Acknowledgements

This work was financially supported by the Chung-Shan Institute of Science and Technology (CSIST) under the Contract No. CSIST-706-V102.

References

Assmann L, JC Bern` ede, A. Drici, C. Amory, E. Halgand, and M. Morsli (2005) Study of the Mo thin films and Mo/CIGS interface properties. Applied Surface Science 246: 159–166.

Dhere MNG (2007) Toward GW/year of CIGS production within the next decade. Solar Energy Materials & Solar Cells 91: 1376–1382.

Dresselhaus S and IL Thomas (2001) Overview Alternative energy technologies. Nature 414: 332–337.

Gordillo G, M Grizalez, and LC Hernandez (1998) Structural and electrical properties of DC sputtered molybdenum films. Solar energy materials and solar cells 51: 327–337.

Green MA, K. Emery, Y. Hishikawa, W. Warta, and E. D. Dunlop (2012) Solar cell efficiency tables (version 39). Prog. Photovolt: Res. 20: 12–20.

Hoffman RA, J. C. Lin, and J. P. Chambers (1991) The effect of ion bombardment on the microstructure and properties of molybdenum films. Thin Solid Films 206: 230–235.

Hsiao KJ, JD Liu, HH Hsieha and TS Jianga (2013) Electrical impact of MoSe2 on CIGS thin-film solar cells. Phys. Chem. Chem. Phys. 15: 18174–18178.

Huang PC, CH Huang, MY Lin, CY Chou, CY Hsu, and CG Kuo (2013) The Effect of Sputtering Parameters on the Film Properties of Molybdenum Back Contact for CIGS Solar Cells. International Journal of Photoenergy 2013: 390824 (8 pages).

Jackson P, D Hariskos, E Lotter, S Paetel, R Wuerz, R Menner, W Wischmann and MY Jeong, CW Kim, DW Park, SC Jung, J Lee, and HS Shim (2011) Field modulation in Na-incorporated Cu(In,Ga)Se2 (CIGS) polycrystalline films influenced by alloy-hardening and pair-annihilation probabilities. Nanoscale Res Lett. 6: 581–586.

Jubault M, L Ribeaucourt, E Chassaing, G Renou, D Lincot, and F Donsanti (2011) Optimization of molybdenum thin films for electrodeposited CIGS solar cells. Solar Energy Materials and Solar Cells 95: S26–S31.

Li ZH, ES Cho, SJ Kwon (2011) Molybdenum thin film deposited by in-line DC magnetron sputtering as a back. Applied Surface Science 257: 9682–9688.

Moons E, T Engelhard, and D Cahen (1993) Ohmic contacts top-CuInSe2 crystals. Journal of Electronic Materials 22: 275–280.

Powalla (2011) New world record efficiency for Cu (In, Ga)Se2 thin□ film solar cells beyond 20%. Prog. Photovolt: Res. Appl. 19: 894–897.

Singh UP and SP Patra (2010) Progress in Polycrystalline Thin-Film Cu(In,Ga)Se2 Solar Cells. International Journal of Photoenergy 2010: 468147 (19 pages).

Thornton JA and DW Hoffman (1989) Stress-related effects in thin films. Thin solid films 171: 5–8.

Wang SF, HC Yang, CF Liu, and HYY Bor (2014) Characteristics of

Bilayer Molybdenum Films Deposited Using RF Sputtering for Back Contact of Thin Film Solar Cells. Advances in Materials Science and Engineering 2014, 531401 (6 pages).

Wu HM, SC Liang, YL Lin (2012) Structure and electrical properties of Mo back contact for Cu(In,Ga)Se2 solar cells. Vacuum 86: 1916–1919.

Yoon JH, S Cho, WM Kimetal. (2011) Optical analysis of the microstructure of a Mo back contact for Cu(In,Ga)Se2 solar cells and its effects on Mo film properties and Na diffusivity. Solar Energy Materials and Solar Cells 95: 959–2964.

Atlas Journal of Materials Science - ISSN 2330-6831. Published By Atlas Publishing, LP (www.atlas-publishing.org)